AD-A066 097 PACIFIC-SIERRA RESEARCH CORP SANTA MONICA CALIF F/G 20/14
AN INTEGRAL-EQUATION APPROACH TO ELF PROPAGATION IN A NON-STRAT--ETC(U)
FEB 79 E C FIELD N00014-78-C-0336

UNCLASSIFIED PSR-904 NL

1 OF 1
ADA
066097

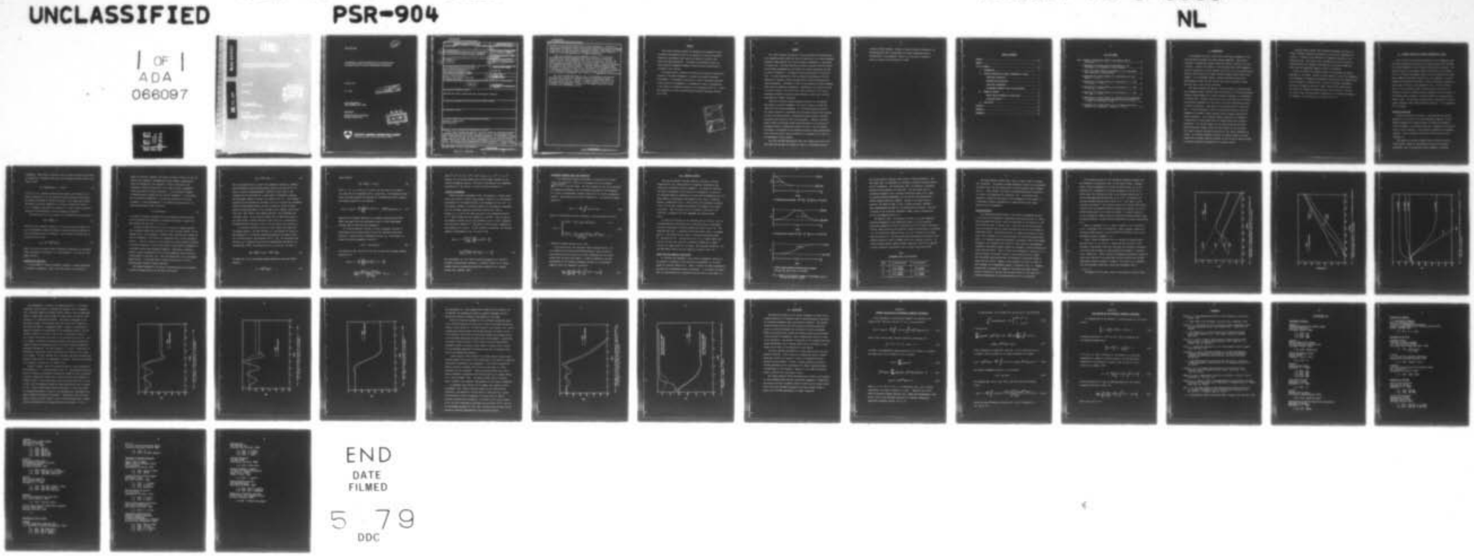

END
DATE
FILMED
5 79
DDC

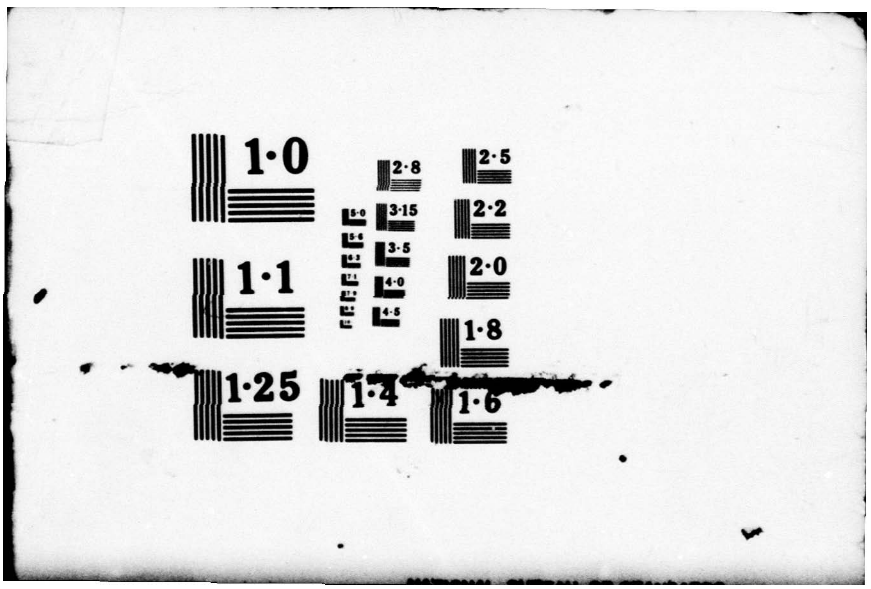
1·0
1·1
1·25
1·4
1·6
1·8
2·0
2·2
2·5
2·8
3·15
3·5
4·0
4·5
5·0
5·6

(12)

PSR Report 904

AN INTEGRAL–EQUATION APPROACH TO ELF PROPAGATION IN A NON–STRATIFIED EARTH–IONOSPHERE WAVEGUIDE

February 1979

E. C. Field

Final Technical Report
Contract N00014–78–C-0336

Sponsored by

OFFICE OF NAVAL RESEARCH
Arlington, Virginia 22217

PACIFIC•SIERRA RESEARCH CORP.
1456 Cloverfield Blvd. Santa Monica, California 90404

UNCLASSIFIED

SECURITY CLASSIFICATION OF THIS PAGE (When Data Entered)

REPORT DOCUMENTATION PAGE

READ INSTRUCTIONS BEFORE COMPLETING FORM

1. REPORT NUMBER

2. GOVT ACCESSION NO.

3. RECIPIENT'S CATALOG NUMBER

(9)

4. TITLE (and Subtitle)

(6) An Integral-Equation Approach to ELF Propagation in a Non-Stratified Earth-Ionosphere Waveguide,

5. TYPE OF REPORT & PERIOD COVERED

Final Technical Report.

6. PERFORMING ORG. REPORT NUMBER

(14) PSR-904

7. AUTHOR(s)

(10) E. C. Field

8. CONTRACT OR GRANT NUMBER(s)

(15) N00014-78-C-0336 new

9. PERFORMING ORGANIZATION NAME AND ADDRESS

Pacific-Sierra Research Corporation
1456 Cloverfield Boulevard
Santa Monica, California 90404

10. PROGRAM ELEMENT, PROJECT, TASK AREA & WORK UNIT NUMBERS

NR 089-129

11. CONTROLLING OFFICE NAME AND ADDRESS

Office of Naval Research
800 North Quincy Street (Code 465)
Arlington, VA 22217

12. REPORT DATE

(11) February 1979

13. NUMBER OF PAGES

29

14. MONITORING AGENCY NAME & ADDRESS (if different from Controlling Office)

(12) 43p.

15. SECURITY CLASS. (of this report)

UNCLASSIFIED

15a. DECLASSIFICATION/DOWNGRADING SCHEDULE

16. DISTRIBUTION STATEMENT (of this Report)

Approved for public release and sale; distribution unlimited.

17. DISTRIBUTION STATEMENT (of the abstract entered in Block 20, if different from Report)

18. SUPPLEMENTARY NOTES

19. KEY WORDS (Continue on reverse side if necessary and identify by block number)

submarine communication
ELF propagation

20. ABSTRACT (Continue on reverse side if necessary and identify by block number)

This report develops and applies a practical method for analyzing long-wave propagation under conditions where the properties of the earth-ionosphere waveguide change markedly over lateral distances comparable to a wavelength or Fresnel zone. Full-wave solutions are used to describe both the vertical and horizontal dependences of the fields, but certain compromises are made to achieve tractability. The method is thus characterized as "quasi-full-wave." Its main limitation is that the equation describing the vertical dependence is assumed to nearly → next page

DD FORM 1473, 1 JAN 73 EDITION OF 1 NOV 65 IS OBSOLETE

UNCLASSIFIED

SECURITY CLASSIFICATION OF THIS PAGE (When Data Entered)

407486 LB

decouple from the equation governing the lateral dependence. The method is valid at any frequency for which waveguide modes describe terrestrial propagation. Nonetheless, its practical utility is probably limited to ELF because the lateral properties of the earth-ionosphere waveguide are usually gradual enough to permit use of the WKB approximation at higher frequencies.

Since the literature provides abundant solutions for the equation describing the vertical dependence, this report focuses on solving the equation for the lateral dependence. To facilitate numerical solution, the lateral equation is transformed into an integral equation that accounts for most full-wave properties, including diffraction around a localized disturbance and reflection from lateral gradients. Numerical solutions based on model disturbances having lateral gradients in the direction of propagation reveal a standing wave pattern in front of the disturbance. The pattern is pronounced if the waveguide properties change substantially over a distance equal to about one-sixth of a wavelength, and is minor if the disturbance is more diffuse.

The often used WKB approximation omits the standing wave pattern and thus gives poor accuracy for regions in front of a disturbance having a relatively abrupt boundary. Because it ignores gradient reflections, the WKB approximation also overestimates the signal transmitted beyond a non-uniformity in the waveguide. However, for all models considered--abrupt or diffuse--the overestimate is minor.

PREFACE

This report develops a method for analyzing the propagation of ELF (extremely low-frequency) waves in the presence of laterally nonuniform ionospheric disturbances that violate the validity criteria of the widely used WKB approximation. The method is particularly useful for calculating ELF propagation anomalies caused by nuclear detonations at altitudes of 30 to 150 km.

The present report continues the Pacific-Sierra Research Corporation's analysis of long-wave propagation in nuclear and naturally disturbed environments. In focusing on the effects of lateral ionospheric gradients in the direction of propagation, it complements an earlier investigation of the effects of gradients transverse to the propagation path (E. C. Field, *ELF Propagation in a Non-Stratified Earth-Ionosphere Waveguide*, PSR 806, April 1978).

SUMMARY

This report develops and applies a practical method for analyzing long-wave propagation under conditions where the properties of the earth-ionosphere waveguide change markedly over lateral distances comparable to a wavelength or Fresnel zone. Full-wave solutions are used to describe both the vertical and horizontal dependences of the fields, but certain compromises are made to achieve tractability. The method is thus characterized as "quasi-full-wave." Its main limitation is that the equation describing the vertical dependence is assumed to nearly decouple from the equation governing the lateral dependence. The method is valid at any frequency for which waveguide modes describe terrestrial propagation. Nonetheless, its practical utility is probably limited to ELF because the lateral properties of the earth-ionosphere waveguide are usually gradual enough to permit use of the WKB approximation at higher frequencies.

Since the literature provides abundant solutions for the equation describing the vertical dependence, this report focuses on solving the equation for the lateral dependence. To facilitate numerical solution, the lateral equation is transformed into an integral equation that accounts for most full-wave properties, including diffraction around a localized disturbance and reflection from lateral gradients. Numerical solutions based on model disturbances having lateral gradients in the direction of propagation reveal a standing wave pattern in front of the disturbance. The pattern is pronounced if the waveguide properties change substantially over a distance equal to about one-sixth of a wavelength, and is minor if the disturbance is more diffuse.

The often used WKB approximation omits the standing wave pattern and thus gives poor accuracy for regions in front of a disturbance having a

relatively abrupt boundary. Because it ignores gradient reflections, the WKB approximation also overestimates the signal transmitted beyond a nonuniformity in the waveguide. However, for all models considered--abrupt or diffuse--the overestimate is minor.

TABLE OF CONTENTS

LIST OF FIGURES

I. INTRODUCTION

The wavelength and first Fresnel zone for ELF waves propagating in the earth-ionosphere waveguide can extend several megameters. Many types of ionospheric irregularities exhibit significant lateral variations over such a distance. Ideally, the effects of such irregularities on ELF propagation should be analyzed by full-wave methods rather than the often used WKB approximations, which work well for higher frequency signals having shorter wavelengths. To our knowledge, however, complete full-wave solutions that simultaneously account for both vertical and lateral ionospheric inhomogeneities have to date proven intractable.

This report develops and applies a practical method for analyzing long-wave propagation under conditions where the properties of the earth-ionosphere waveguide change markedly over lateral distances comparable to a wavelength or Fresnel zone. Full-wave solutions are used to describe both the vertical and horizontal dependences of the fields, but certain compromises are made to achieve tractability. The method is thus characterized as "quasi-full-wave." Its main limitation is that the equation describing the vertical dependence is assumed to nearly decouple from the equation governing the lateral dependence. That assumption appears reasonable for ionospheric irregularities of large enough extent to significantly affect long-wave propagation. The vertical equation can be solved using the well-known method developed by Budden (*1961a*) and often applied in the literature. This report focuses on solving the equation for the lateral dependence of fields. To facilitate numerical solution, the lateral equation is transformed into an integral equation analogous to that derived by Hufford (*1952*) to describe ground-wave propagation over irregular terrain.

A previous report (*Field, 1978*) developed approximate solutions for a weak, localized ionospheric disturbance remote from the transmitter and receiver. It pointed up the importance of gradients transverse to the propagation path. The present report complements the earlier results by giving solutions for ionospheric disturbances of arbitrary strength and extent that are azimuthally symmetric about the transmitter.

Section II derives the integral equation that describes the lateral dependence of the fields. Section III gives numerical results for propagation in the presence of ionospheric disturbances centered over the transmitter and over the midpath of a long ELF link. Several of the model disturbances represent environments produced by single, high-altitude nuclear bursts. All results are compared with WKB solutions, and the effects of varying the lateral scale size and boundary diffuseness of the assumed disturbances are examined. The conclusions are presented in Sec. IV.

II. INTEGRAL EQUATION FOR LATERAL DEPENDENCE OF FIELDS

First we review the well-known equations for ELF propagation under stratified conditions, then derive the integral equation that describes the lateral dependence of the fields for nonstratified conditions. Two simpler versions of the integral equation are derived for the special cases of a localized disturbance remote from the terminals and an azimuthally symmetric disturbance centered over the transmitter. To avoid mathematical complexities unrelated to lateral ionospheric gradients, we ignore earth curvature and the geomagnetic field. The first approximation is well justified at ELF; the second yields results that are reasonably accurate for ambient daytime conditions and very accurate for disturbances where ionospheric reflection heights are depressed below ambient levels. The equations derived below are inappropriate for estimating propagation under normal nighttime conditions. A time dependence $e^{i\omega t}$ is assumed.

STRATIFIED CONDITIONS

We begin by defining a function, ψ, that describes the lateral dependence of the fields in the earth-ionosphere waveguide. For ELF TEM-mode propagation at ranges exceeding the effective ionospheric reflection height, ψ could denote either the z component of the electric field or vector potential, or the horizontal component of the magnetic intensity. Here we associate ψ with the vertical electric-field component, E.

ELF signals are typically radiated from a horizontal electric dipole antenna. Hence the fields have both radial and azimuthal dependences, even if the earth-ionosphere waveguide is laterally homogeneous. Under typical conditions, then, the wave equation can be solved by separation of variables, which gives the following well-known result (e.g., *Galejs, 1972*):

$$E_0 = A\Lambda_0 F_0(z)\psi_0(r,\theta) \quad \text{volts/m} \quad . \tag{1}$$

In Eq. (1) A is a constant involving dipole moment, wave frequency, and ground conductivity; Λ_0 is the excitation factor describing the efficiency with which the TEM mode is launched; and $F_0(z)$ is the height-gain function describing the vertical dependence of the field, normalized to unity at $z = 0$. Throughout this report the subscript 0 is used to denote quantities associated with undisturbed, laterally homogeneous conditions.

The function ψ_0 in Eq. (1) satisfies the two-dimensional wave equation

$$(\nabla_T^2 + k^2 S_0^2)\psi_0 = 0 \quad , \tag{2}$$

where ∇_T^2 is the transverse Laplacian, k is the free-space wave number, and S_0 is a propagation constant determined by imposing boundary conditions on F_0 at the ground and in the ionosphere. For stratified conditions, Eq. (2) is easily solved to give

$$\psi_0 = \cos\theta \; S_0 H_1^{(2)}(kS_0 r) \quad , \tag{3}$$

where r and θ are the usual circular cylindrical coordinates; the horizontal dipole transmitter is located at $r = 0$ and oriented at $\theta = 0$; and H is the Hankel function.

NONSTRATIFIED CONDITIONS

In the presence of lateral ionospheric gradients a rigorous separation of variables is impossible. Hence, the fields cannot be expressed as a product of vertical, azimuthal, and radial functions as in Eqs. (1) and (3). However, for ionospheric inhomogeneities large enough to significantly affect ELF propagation, scale lengths for lateral variations of the ionospheric refractive index tend to be at least an order of magnitude larger than those for vertical variations. It can therefore be argued on semiquantitative grounds that the vertical dependence, F, of the fields and the associated eigenvalue, S, are governed primarily by the local ionosphere. In this approximation it is assumed by analogy with Eq. (1) that the ground-level field is given by

$$E \approx A\Lambda(x,y)\psi(x,y) \quad . \tag{4}$$

To account for lateral variations that are nonsymmetric about the source, we have switched from cylindrical to Cartesian coordinates. Equation (4) also reflects the fact that $F = 1$ at $z = 0$.

To find the field from Eq. (4), we use a mixture of eikonal and full-wave techniques perhaps best described as a "quasi-full-wave" method. By the arguments above, the ionosphere is assumed locally stratified for finding the vertical dependence of the fields, the eigenvalue $S(x,y)$, and the excitation factor, Λ. Thus the equation for these quantities, and the method of solution, are formally identical to those widely applied in analyzing ELF propagation in a laterally uniform earth-ionosphere waveguide. They differ in practice, however, because the equation for the vertical dependence must be solved at a large number of locations, (x,y), each characterized by a local ionospheric height-profile. On the other hand, a single solution suffices for all locations under laterally uniform conditions.

The lateral dependence of the field is expressed mainly in the function ψ, which by analogy with Eq. (2) satisfies the equation

$$(\nabla_T^2 + k^2 S^2(x,y))\psi = 0 \quad . \tag{5}$$

The local eigenvalue $S(x,y)$, unlike the propagation constant S_0, exhibits spatial dependence, which precludes general analytic solutions of Eq. (5). $S(x,y)$ is found by imposing boundary conditions on the fields in the ionosphere and at the ground for a large number of geographic locations, thus obtaining a matrix of values to be entered in Eq. (5). The literature supplies full-wave methods for obtaining S and Λ for virtually any ionospheric refractive-index height-profile, as well as numerical results for many ambient and disturbed models of the ionosphere (e.g., *Budden, 1961a; Field, 1970; Wait, 1970; Galejs, 1972; Pappert and Moler, 1974; Greifinger and Greifinger, 1978*). We can therefore assume that all quantities except ψ are either known or readily obtainable, which allows us to concentrate on obtaining full-wave solutions of Eq. (5) for the lateral wave function, ψ.

To facilitate numerical solution, we first recast the problem into an integral equation. Our main interest is in calculating the effects on ELF propagation of a laterally nonuniform ionospheric disturbance, which can be characterized by the difference $S^2(x,y) - S_0^2$. The undisturbed wave function, ψ_0, is governed by S_0 and can be assumed known through Eq. (3). Following Wait (*1964*), the subtraction of Eq. (2) from Eq. (5) leads to

$$(\nabla_T^2 + k^2 S_0^2)\ (\psi - \psi_0) = -k^2[S^2 - S_0^2]\psi \quad . \tag{6}$$

We convert Eq. (6) to the desired integral equation by using the Green's function,

$$G = -i\pi H_0^{(2)}(kS_0 r_2) \quad , \tag{7}$$

which satisfies

$$(\nabla_T^2 + k^2 S_0^2)G = -4\pi\delta(r_2) \quad , \tag{8}$$

where $r_2 = |\underline{r} - \underline{r}_1|$ ($\underline{r}$ and $\underline{r}_1$ are vectors from the origin to the observation point and to an integration point, respectively). By following the usual Green's function procedure and applying the two-dimensional Green's theorem, the integral equation for ψ is obtained:

$$\psi(x,y) = \psi_0(x,y) - \frac{ik^2}{4}\iint_{-\infty}^{\infty} dx'dy'[S^2(x',y') - S_0^2]H_0^{(2)}(kS_0r_2)\psi(x',y') \ . \tag{9}$$

Equation (9) is formally identical to an integral equation given by Wait (*1964*), who used first-order perturbation theory to obtain approximate solutions valid at VLF (very low frequencies).

It is also convenient to define a relative propagation function, W, which denotes the fractional amount by which the disturbed lateral wave function, ψ, differs from the undisturbed function, ψ_0. Specifically, we define the relative propagation function by

$$\psi(x,y) \equiv W(x,y)\psi_0(x,y) \quad . \tag{10}$$

The insertion of Eqs. (10) and (3) into Eq. (9) gives the following integral equation for W:

$$W(x,y) = 1 - \frac{ik^2}{4}\iint_{-\infty}^{\infty} dx'dy'\left[S^2(x',y') - S_0^2\right]$$

$$\cdot\left[\frac{x'r}{xr_1}\right] \frac{H_0^{(2)}(kS_0r_2)\ H_1^{(2)}(kS_0r_1)}{H_1^{(2)}(kS_0r)}\ W(x',y') \quad , \tag{11}$$

where $r^2 = x^2 + y^2$, $r_1^2 = (x')^2 + (y')^2$, and $r_2 = (x - x')^2 + (y - y')^2$. Equation (11) is the most general form of the integral equation for the relative propagation function. Note that in the absence of an ionospheric disturbance, $S^2 = S_0^2$ and Eq. (11) has the trivial solution $W = 1$.

LOCALIZED DISTURBANCES

Despite the great wavelengths at ELF, the distance, r, between transmitter and receiver is usually large enough to permit use of the asymptotic approximation for the Hankel function in the denominator of Eq. (11). In the numerator, however, the validity condition on the asymptotic approximation for the Hankel functions is much more restrictive. That is because r_1 or r_2 can be very small over part of the integration interval if $S^2 - S_0^2$ is nonzero near the transmitter or receiver. Thus, we may use the asymptotic formula only if the disturbance occurs at least a megameter away from either terminal; $S^2 - S_0^2$ cannot be nonzero within a megameter of the transmitter or receiver. If that condition is satisfied, the following asymptotic approximation of Eq. (11) may be used:

$$W(x,y) = 1 + \frac{k^{3/2} e^{-\pi i/4}}{2\sqrt{2\pi S_0}} \iint_{-\infty}^{\infty} dx'dy' \left[S^2 - S_0^2\right]$$

$$\cdot \left[\frac{r}{r_1 r_2}\right]^{\frac{1}{2}} \left[\frac{x'r}{xr_1}\right] \exp\left\{-ikS_0\left[r_1 + r_2 - r\right]\right\} \quad . \tag{12}$$

Not surprisingly, Eq. (12), which describes propagation in a laterally irregular earth-ionosphere waveguide, is formally similar to the classic integral equation representing ground-wave propagation over irregular terrain (e.g., *Hufford, 1952*).

DISTURBANCE SYMMETRIC ABOUT THE TRANSMITTER

If an azimuthally symmetric disturbance is centered over the transmitter, the quantity $S^2 - S_0^2$ in Eq. (9) depends only on the distance, $\sqrt{(x')^2 + (y')^2}$, from the origin. For that situation Eq. (9) can be rewritten in cylindrical coordinates, and the azimuthal dependence can be integrated out to give a one-dimensional integral equation for the relative propagation function. (The procedure is outlined in Appendix A.) The resulting integral equation is

$$W(r) = 1 - \frac{ik^2\pi}{2} \int_0^\infty dr' K(r,r')W(r') \quad , \tag{13a}$$

where r is the distance from the transmitter to the observation point and

$$K(r,r') = \begin{cases} r'[S^2(r') - S_0^2]\,J_1(kS_0r')H_1^{(2)}(kS_0r') & r' \le r \\ \\ \dfrac{r'[S^2(r') - S_0^2]\,J_1(kS_0r)H_1^{(2)}(kS_0r')H_1^{(2)}(kS_0r')}{H_1^{(2)}(kS_0r)} & r' \ge r \end{cases} \quad . \tag{13b}$$

J denotes the Bessel function in Eq. (13b).

In the next section, the full-wave results computed from Eq. (13) are compared with the often used WKB approximation, which is valid at large distances from the source for lateral inhomogeneities with scales greater than an inverse wave number. As shown in Appendix B, the WKB approximation of the relative propagation function for a disturbance symmetric about the transmitter is given by

$$W_{WKB}(r) \sim \frac{S(r = 0)}{\left[S_0S(r)\right]^{1/2}} \exp\left[-ik \int_0^r [S(r') - S_0]\,dr'\right] \quad . \tag{14}$$

III. NUMERICAL RESULTS

This section presents full-wave numerical solutions of the one-dimensional Eq. (13), which applies to ionospheric disturbances that depend only on distance from the transmitter. The solutions illustrate the effects of gradients in the direction of propagation. We have not yet developed numerical procedures for solving the two-dimensional Eq. (11), which applies to disturbances that depend on both lateral coordinates. However, as mentioned in Sec. I, Field (*1978*) gives approximate solutions of Eq. (12) for weak, localized disturbances that depend on two lateral coordinates. Those solutions pertain to gradients transverse to the direction of propagation and thus complement the solutions given below.

To check on the accuracy of the algorithm used to solve Eq. (13), we performed numerical calculations for two idealized types of disturbance for which ψ (and hence W) could be analytically found from Eq. (5). The idealized types are 1) a laterally uniform disturbance where S is independent of r but differs from S_0, and 2) a nonuniform disturbance where $S^2 - S_0^2$ varies as $1/r^2$. The solution to Eq. (5) is a simple Hankel function for the first test case and a complicated combination of Hankel functions of complex order for the second. Both solutions satisfy Eq. (13) and agree almost exactly with the numerical solutions of Eq. (13).

MODELS USED FOR NUMERICAL CALCULATIONS

To illustrate the dependence of the relative propagation function on the severity of gradients in the direction of propagation, we use three simple but realistic models for S. Figure 1 depicts the models schematically and gives the corresponding analytic expressions. In each model the disturbance is characterized by an exponential function with a scale length, Δr,

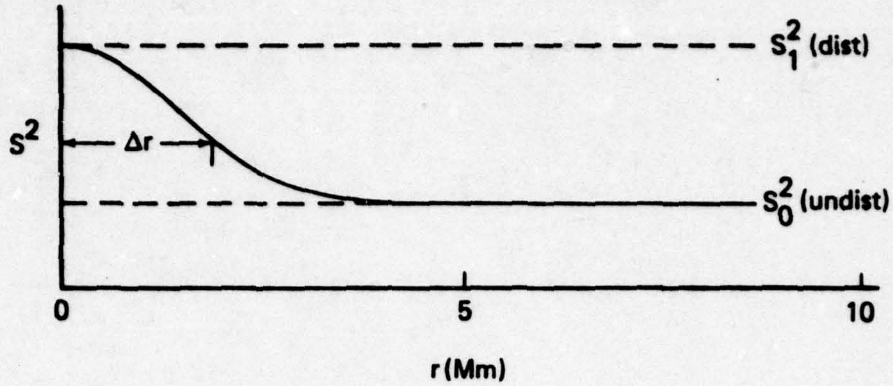

a: Disturbance over transmitter $\left((S^2 - S_0^2) = (S_1^2 - S_0^2)\ \exp(-r^2/(\Delta r)^2)\right)$

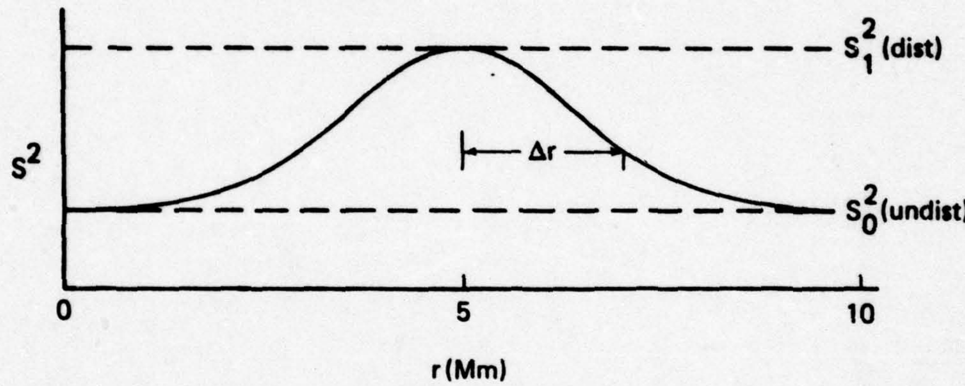

b: Disturbance over midpath $\left((S^2 - S_0^2) = (S_1^2 - S_0^2)\ \exp(-(r-5)^2/(\Delta r)^2)\right)$

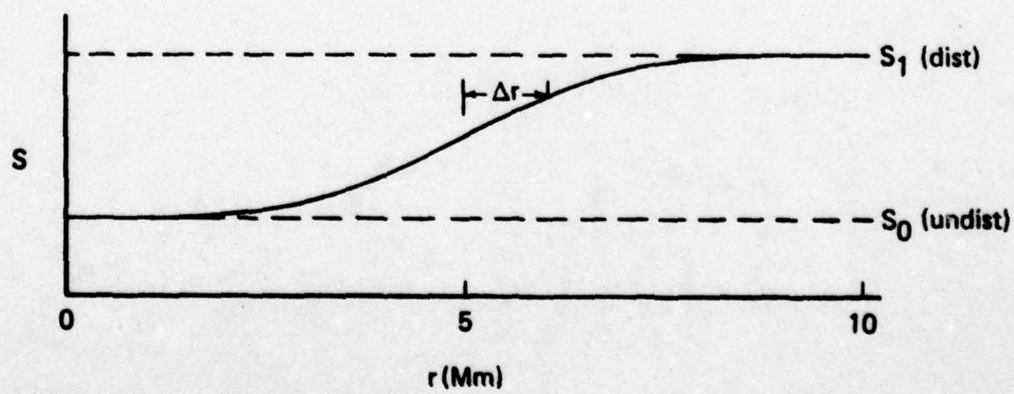

c: Uniform regions separated by diffuse boundary at midpath

$\left((S - S_0) = (S_1 - S_0)/(1+\exp[-(r-5)/\Delta r])\right)$

Fig. 1--Models of azimuthally symmetric disturbances used in calculations (not to scale).

that can be varied to indicate either abrupt or diffuse boundaries. The first model (Fig. 1a) represents an ionospheric depression centered directly over the transmitter. The second model (Fig. 1b) represents a depression centered over the midpath of a 10-Mm link. The third model (Fig. 1c) represents propagation from a uniformly undisturbed region into a region of uniformly depressed ionosphere, the two regions being separated by a diffuse boundary centered at midpath. Because of the large radius of curvature, the models in Figs. 1b and 1c should reasonably represent a plane waveguide-mode incident on a one-dimensional disturbance. Note that a lowering of the "effective" ionospheric height usually increases both the real and imaginary parts of S.

The symbols in Fig. 1 are defined as follows: S_0 is the eigenvalue governing propagation in the undisturbed region; S_1 is the eigenvalue governing propagation at the most disturbed point; and Δr (Mm) is the characteristic length over which the conditions change from undisturbed to disturbed, i.e., S(r) effectively changes from S_0 to S_1 over a distance two or three times as large as Δr. The table below shows the numerical values and corresponding attenuation rates (in dB/Mm) used for the constants S_0 and S_1. S_0 values represent nominal ambient daytime conditions; those for S_1 represent a severe ionospheric disturbance, such as a major solar proton event.

Table

PARAMETERS USED IN CALCULATIONS

f(Hz)	S_0 (undisturbed)	S_1 (disturbed)
45	1.2 - 0.08 i (0.65 dB/Mm)	1.75 - 0.3 i (2.4 dB/Mm)
75	1.15 - 0.085 i (1.15 dB/Mm)	1.5 - 0.25 i (3.4 dB/Mm)

The simple analytic forms in Fig. 1 are, of course, used for interpretive convenience. The numerical methods employed to obtain the corresponding solutions to Eq. (13) work equally well for any disturbance where S depends only on r. Then, however, S(r) must be calculated numerically and entered as a table to the algorithm for solving Eq. (13). To illustrate this capability, results are also given for ELF propagation in the presence of a disturbance created by detonation of a high-altitude nuclear weapon directly over the transmitter.

CALCULATED RESULTS

All results given below pertain to the relative propagation function, W, the ratio of the disturbed to undisturbed radial wave function, ψ. Recall that the ground-level electric field is proportional to the product of ψ and the excitation factor, Λ (see Eq. (4)). W does not contain the excitation factor and therefore does not always represent the ratio of the disturbed to undisturbed fields. The excitation factor is roughly proportional to the inverse of the thickness (i.e., effective height) of the earth-ionosphere waveguide. For laterally nonuniform waveguides, the geometric mean of the inverse thickness at the transmitter and receiver is often used as an approximation. Ionospheric disturbances usually depress the ionosphere, thereby increasing the local excitation factor. Thus, if either the transmitter or receiver is in a disturbed region, as in Figs. 1a and 1c, the excitation factor is larger than the ambient value and the ratio of disturbed to undisturbed fields is larger than the ratio W. However, W does represent the ratio of fields if both terminals are in undisturbed regions, as depicted in Fig. 1b. Regarded heuristically, W accounts for changes in attenuation and phase velocity, whereas Λ accounts for the fact that the power density in the wavefront is inversely proportional to the cross-sectional area of the waveguide.

The calculated results for the ionospheric depression centered over the transmitter, illustrated in Fig. 1a, are shown in Figs. 2 through 4. Figure 2 shows the magnitude of W versus the lateral scale, Δr, of the depression for a pathlength of 10 Mm and frequencies of 45 and 75 Hz. Curves depict the full-wave solutions to the integral equation (Eq. 13) and the approximate WKB solution given by Eq. (14). As expected, the full-wave and WKB solutions agree closely if $\Delta r > \lambda/2\pi$, where λ is the free-space wavelength.* This condition satisfies the familiar WKB validity criterion that the waveguide properties change only slightly over a horizontal distance equal to an inverse wave number. For smaller values of Δr that correspond to highly localized disturbances having relatively large horizontal gradients, the WKB solutions significantly overstate the magnitude of W.

Figure 3, analogous to Fig. 2, shows the phase of W as a function of Δr for a disturbance over the transmitter. Again, agreement between the full-wave and WKB solutions is good provided the horizontal scale of the disturbance exceeds a megameter or so.

Figure 4 shows the magnitude of W as a function of distance rather than scale size, Δr, as in Fig. 2. Recall that W is the ratio of the disturbed to undisturbed radial wave functions, and increases or decreases in electric-field strength are characterized by W's greater or less than unity, respectively. Figure 4 shows that widespread disturbances (large Δr) cause a net reduction in the radial wave function, whereas more confined disturbances actually increase it slightly. (Of course, as Δr approaches zero the disturbance essentially ceases and W approaches unity.)

---

*The quantity $\lambda/2\pi$ is about 1 Mm at 45 Hz and about 0.6 Mm at 75 Hz.

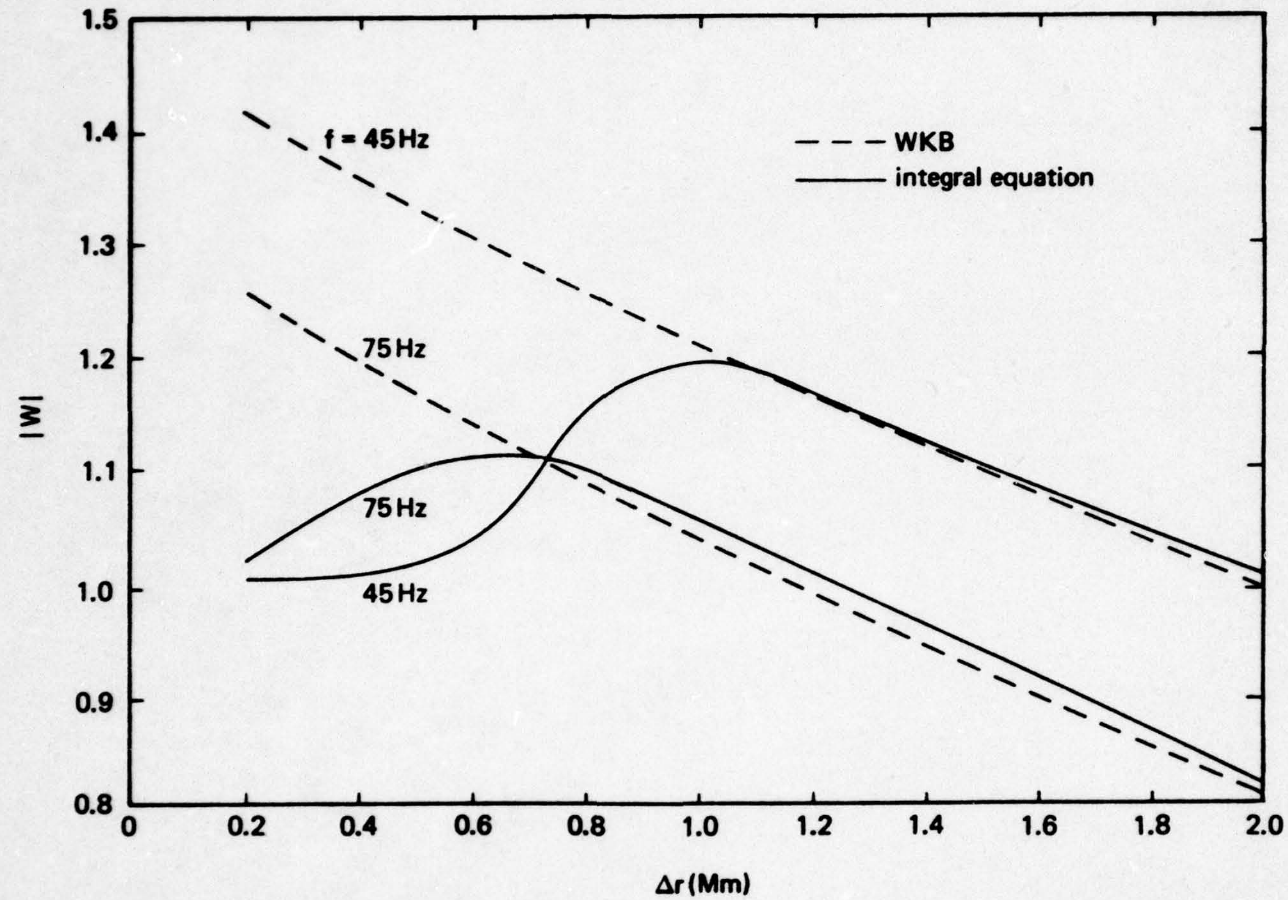

Fig. 2--Amplitude of W versus éffective half-width, Δr, for disturbance over transmitter, 10-Mm pathlength (see Fig. 1a and table).

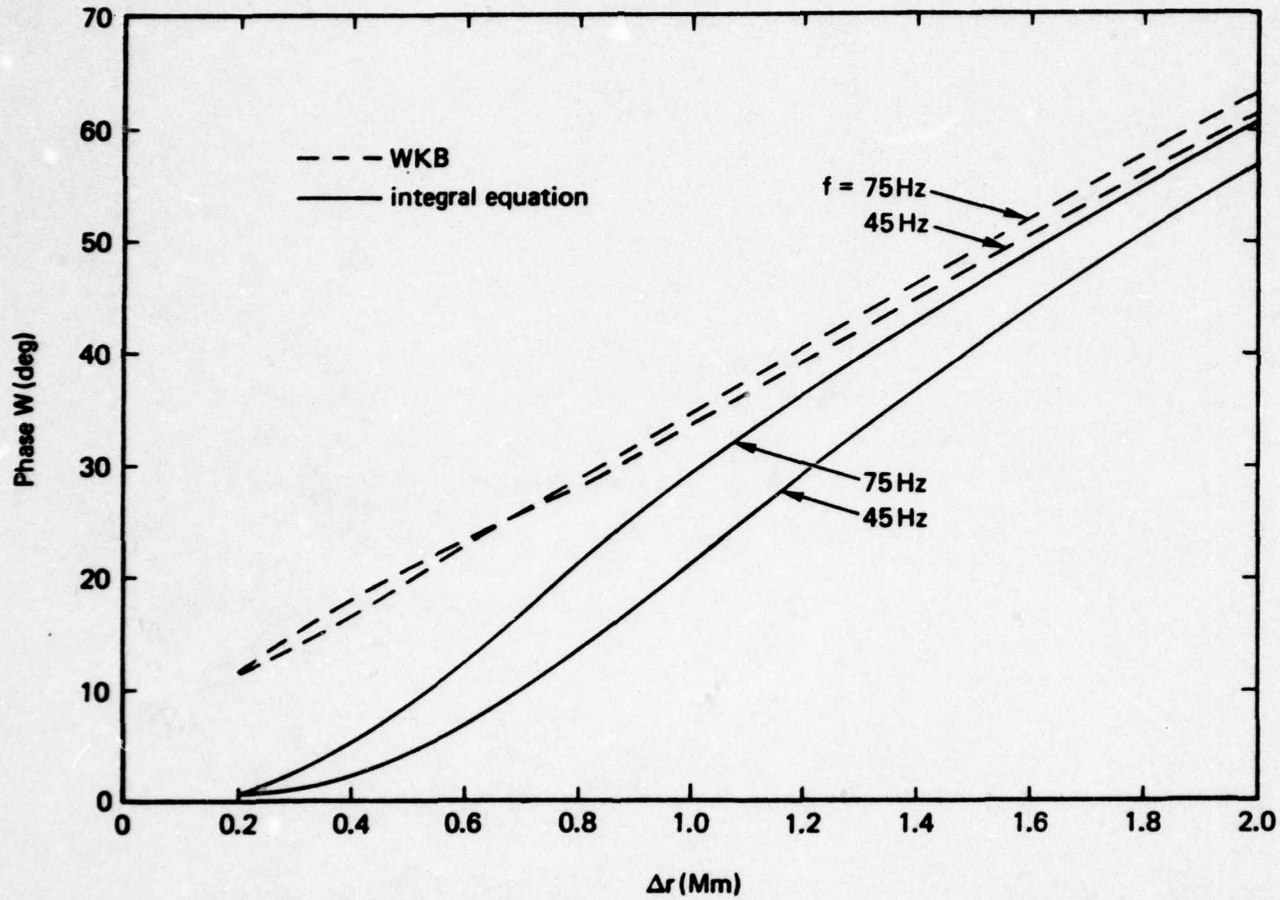

Fig. 3--Phase of W versus effective half-width, Δr, for disturbance over transmitter, 10-Mm pathlength (see Fig. 1a and table).

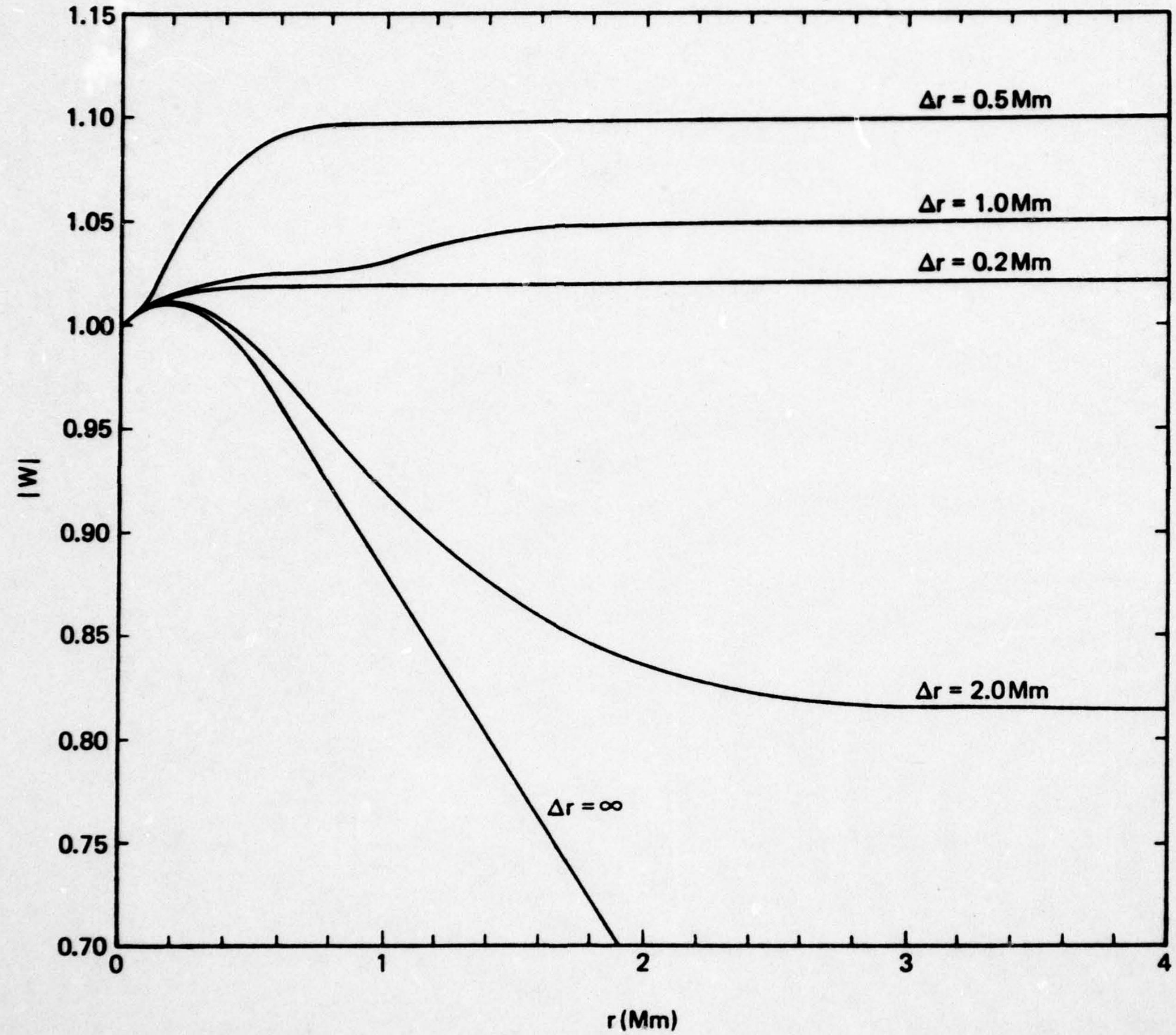

Fig. 4--Amplitude of W versus distance for disturbance over transmitter, f = 75 Hz (see Fig. 1a and table).

This phenomenon is a result of two competing factors: 1) increased attenuation, which causes W to decrease with distance, and 2) propagation from a disturbed region of low-phase velocity (large S) into an undisturbed region of higher phase velocity (small S), which causes the electric field, and hence W, to increase with distance. The latter is analogous to the well-known increase of the electric field that occurs with a reduction in the refractive index of a propagation medium. Clearly, the importance of anomalous attenuation is proportional to the pathlength exposed to the disturbance, whereas any increase in the electric field depends mainly on the contrast between phase velocities at the transmitter and receiver. Thus, W is slightly increased by localized disturbances with small exposed pathlengths, whereas the degrading effects of increased attenuation dominate in widespread disturbances. The curve labeled $\Delta r = \infty$ in Fig. 4 shows how W is affected by a horizontally uniform disturbance (the value S_1 in the table) at all ranges. For this limiting case, W decreases essentially monotonically because the phase velocity is independent of distance, whereas the attenuation rate everywhere increases over the ambient value.

Figures 5 through 7 show the calculated values of W versus distance for the disturbance at r = 5 Mm illustrated in Fig. 1b. These figures portray the effects of making the disturbance progressively broader and hence less abrupt. A distinct standing wave pattern due to reflections from the disturbance is evident in Figs. 5 and 6, which show results for the two cases (Δr = 0.2 and 0.5 Mm) where the waveguide properties change substantially over a distance of $\lambda/2\pi$. Since the WKB solution ignores reflections, it incorrectly omits the standing wave pattern in front of the disturbance and overestimates the signal transmitted through the disturbance. Nevertheless, even for disturbances as abrupt as those in Figs. 5 and 6, the WKB solution gives a remarkably good approximation of the signal behind the disturbance. In Fig. 7

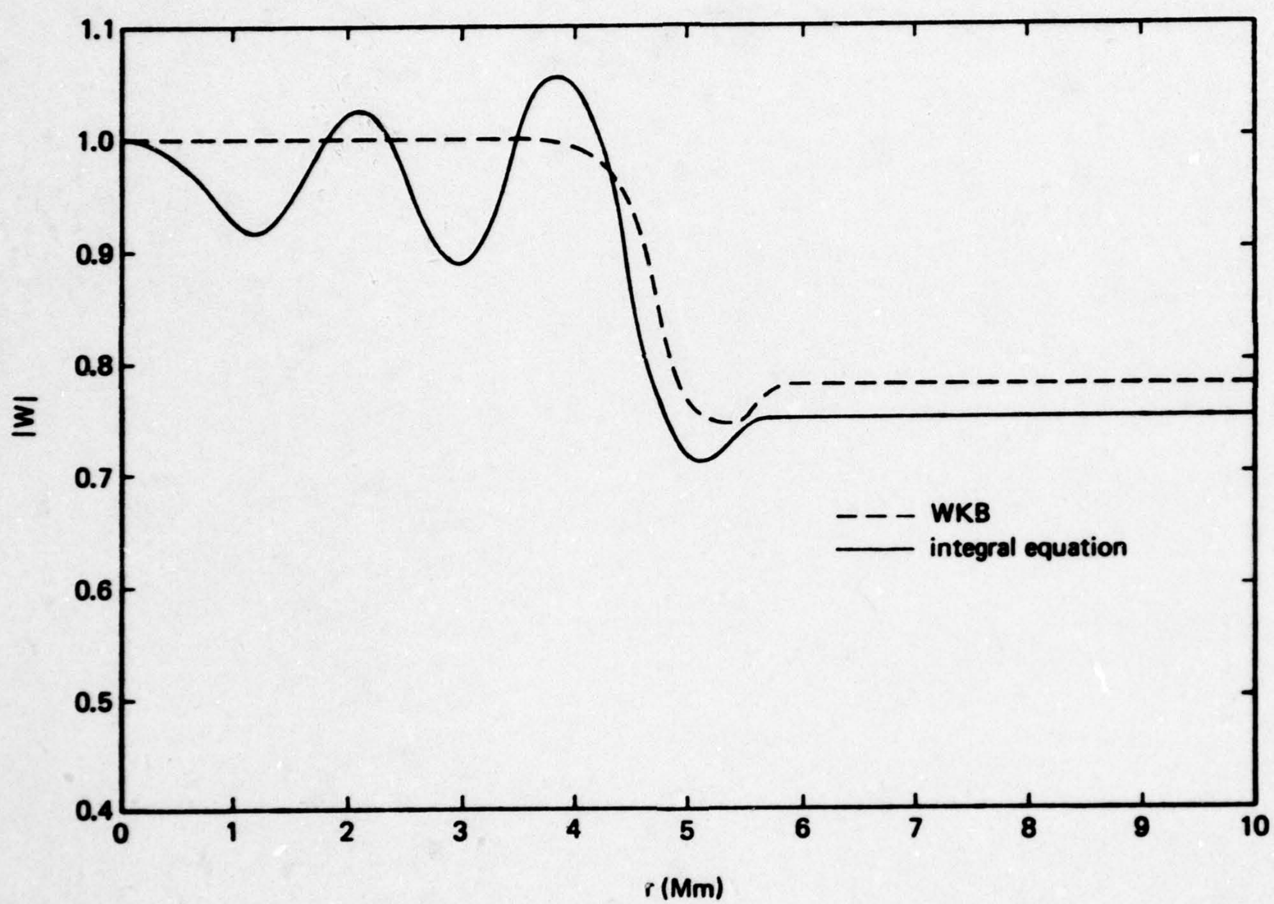

Fig. 5--Amplitude of W versus distance for disturbance at r = 5 Mm: Δr = 0.2 Mm, f = 75 Hz (see Fig. 1b and table).

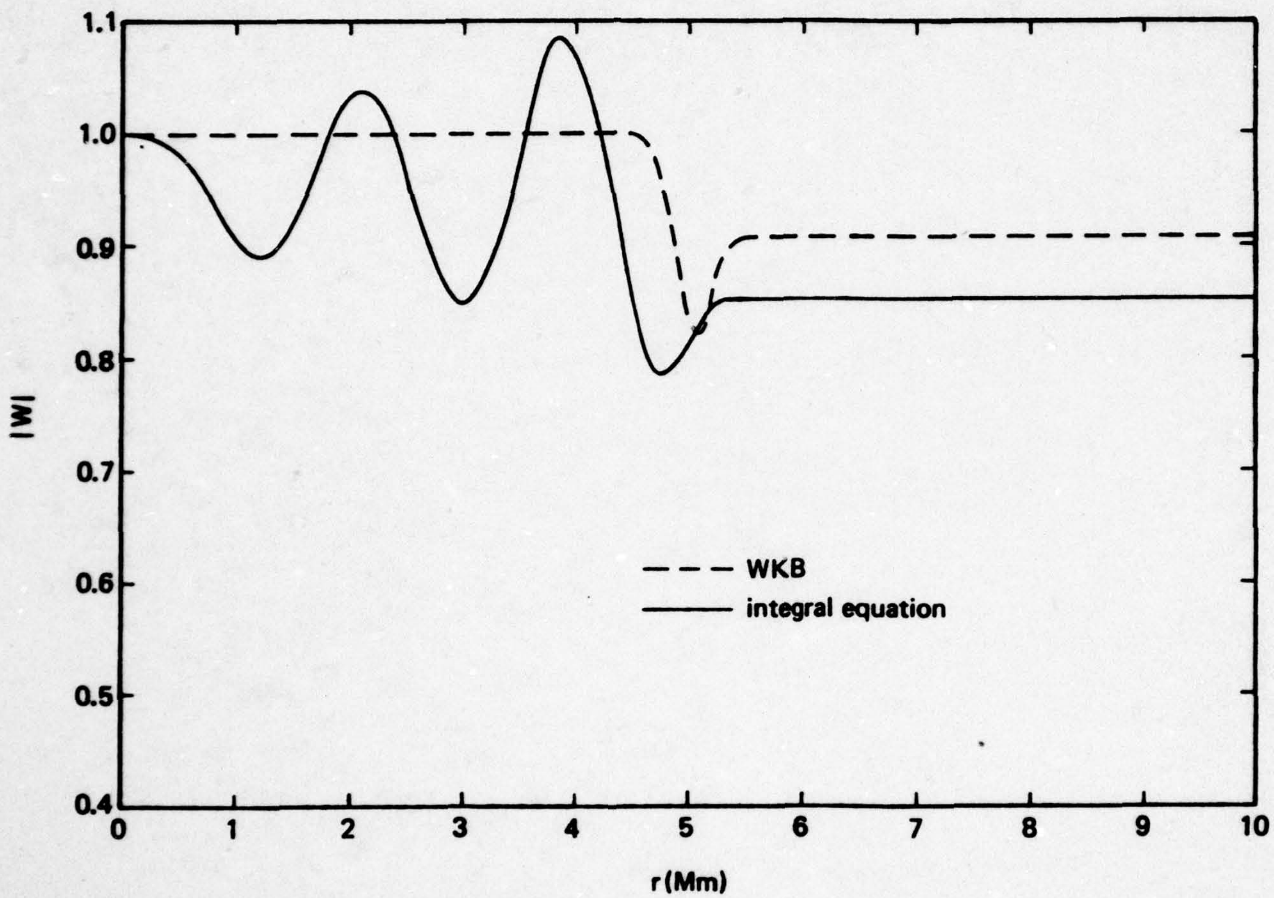

Fig. 6--Amplitude of W versus distance for disturbance at $r = 5$ Mm: $\Delta r = 0.5$ Mm, $f = 75$ Hz (see Fig. 1b and table).

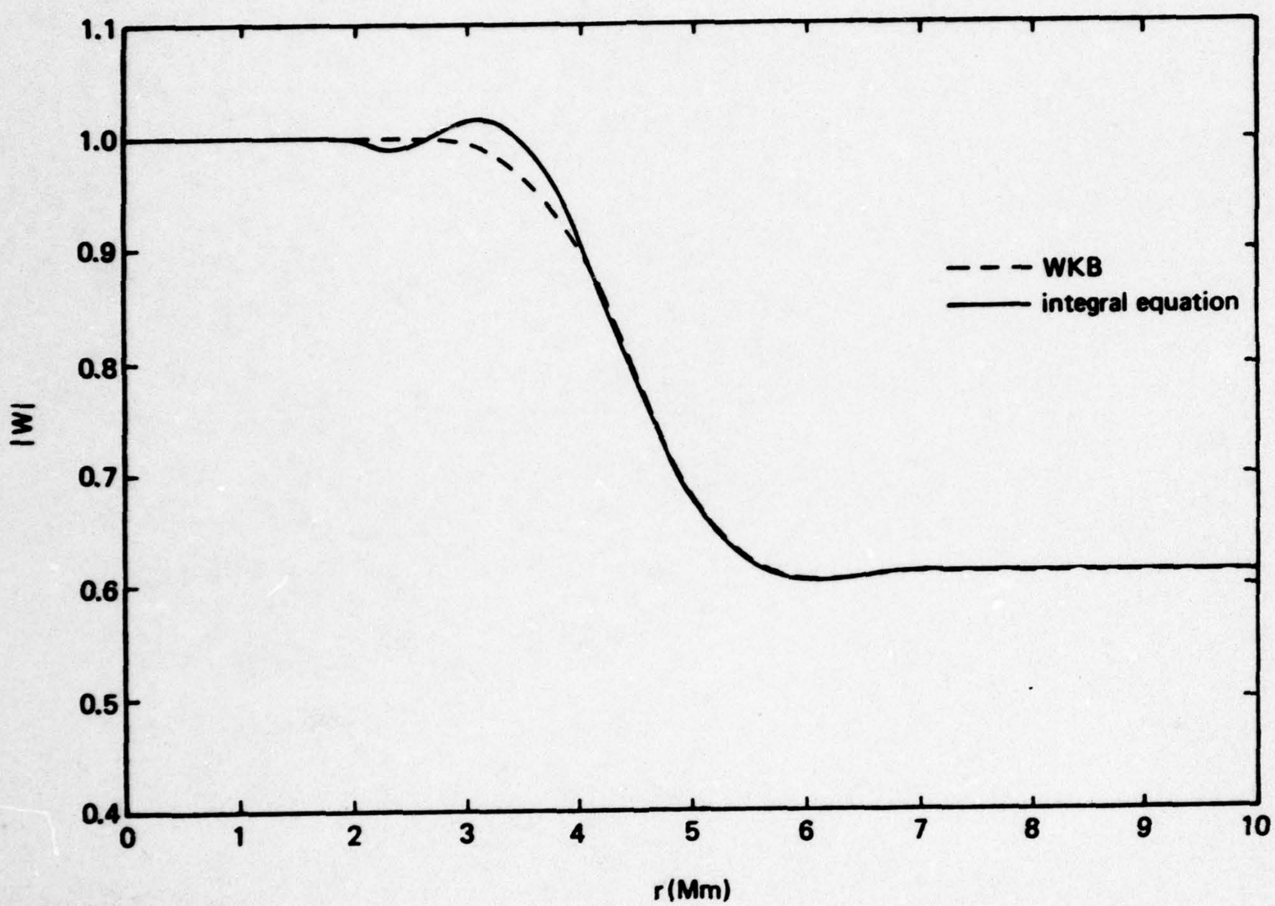

Fig. 7--Amplitude of W versus distance for disturbance at r = 5 Mm: Δr = 1 Mm, f = 75 Hz (see Fig. 1b and table).

the disturbance ($\Delta r = 1$ Mm) changes fairly slowly over the distance $\lambda/2\pi$. As expected, the standing wave pattern is greatly diminished, and the WKB solution affords an excellent approximation at all ranges.

Figure 8 illustrates propagation from a uniformly undisturbed region into a uniformly disturbed one (see Fig. 1c) where the boundary between the regions is quite abrupt ($\Delta r = 0.2$ Mm) relative to the distance $\lambda/2\pi$. Again, a standing wave pattern--absent from the WKB solution--is evident in front of the boundary, and W falls off monotonically behind the boundary because of the increased attenuation associated with the disturbance. Calculations performed for models similar to that in Fig. 1c but with more diffuse boundaries (larger Δr) produce results similar to those in Fig. 8 except for the diminished importance of reflections and the corresponding reduction of the standing wave intensity.

A final purpose of this analysis is to assess whether lateral nonuniformities impair the accuracy of WKB calculations of the effects of high-altitude nuclear detonations on ELF propagation. Field (*1978*) evaluates the effects of bursts at midpath; here we focus on the effect of a burst detonated over the transmitter. Bursts at altitudes below, say, 150 km produce ionospheric disturbances with lateral scales up to perhaps 1500 km (e.g., *Field and Engel, 1965*). The analytic models used to calculate Figs. 2 through 4 are reasonably representative of that range of parameters.

To supplement those results, and to examine less idealized nuclear environments, Fig. 9 shows calculated results for two nominal bursts producing 1) two megatons of fisison debris at 300 km altitude 1 minute after detonation, and 2) two megatons of fission debris at 1000 km altitude 10 minutes after detonation. The values of S(r) used as inputs to Eq. (13) were calculated by Greifinger and Greifinger (*1977*). Even for the low assumed frequency of 45 Hz, Fig. 9 indicates that the WKB solution affords an excellent approximation of the full-wave solution.

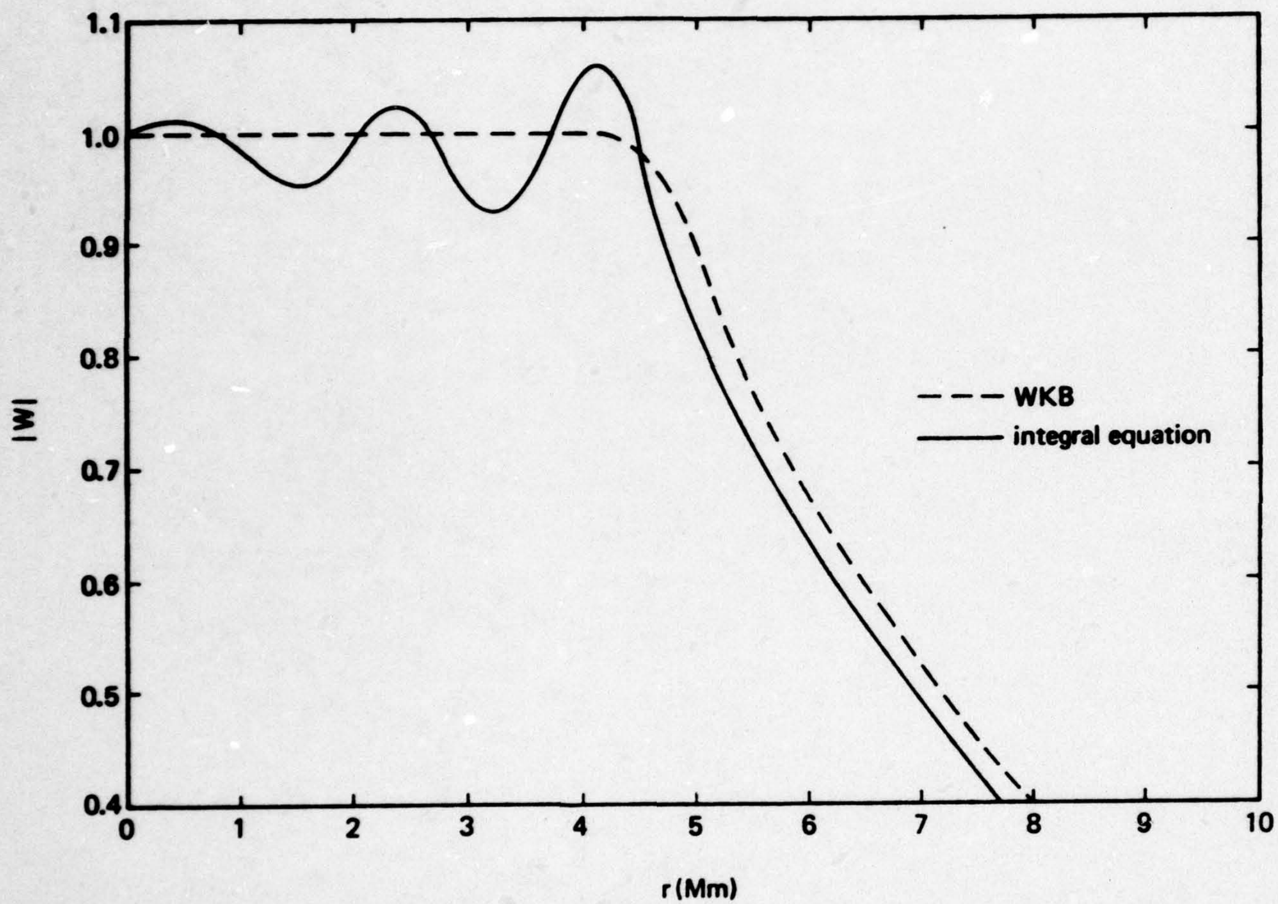

Fig. 8--Amplitude of W versus distance for propagation from undisturbed to disturbed uniform regions separated by diffuse boundary at $r = 5$ Mm: $\Delta r = 0.2$ Mm, $f = 75$ Hz (see Fig. 1c and table).

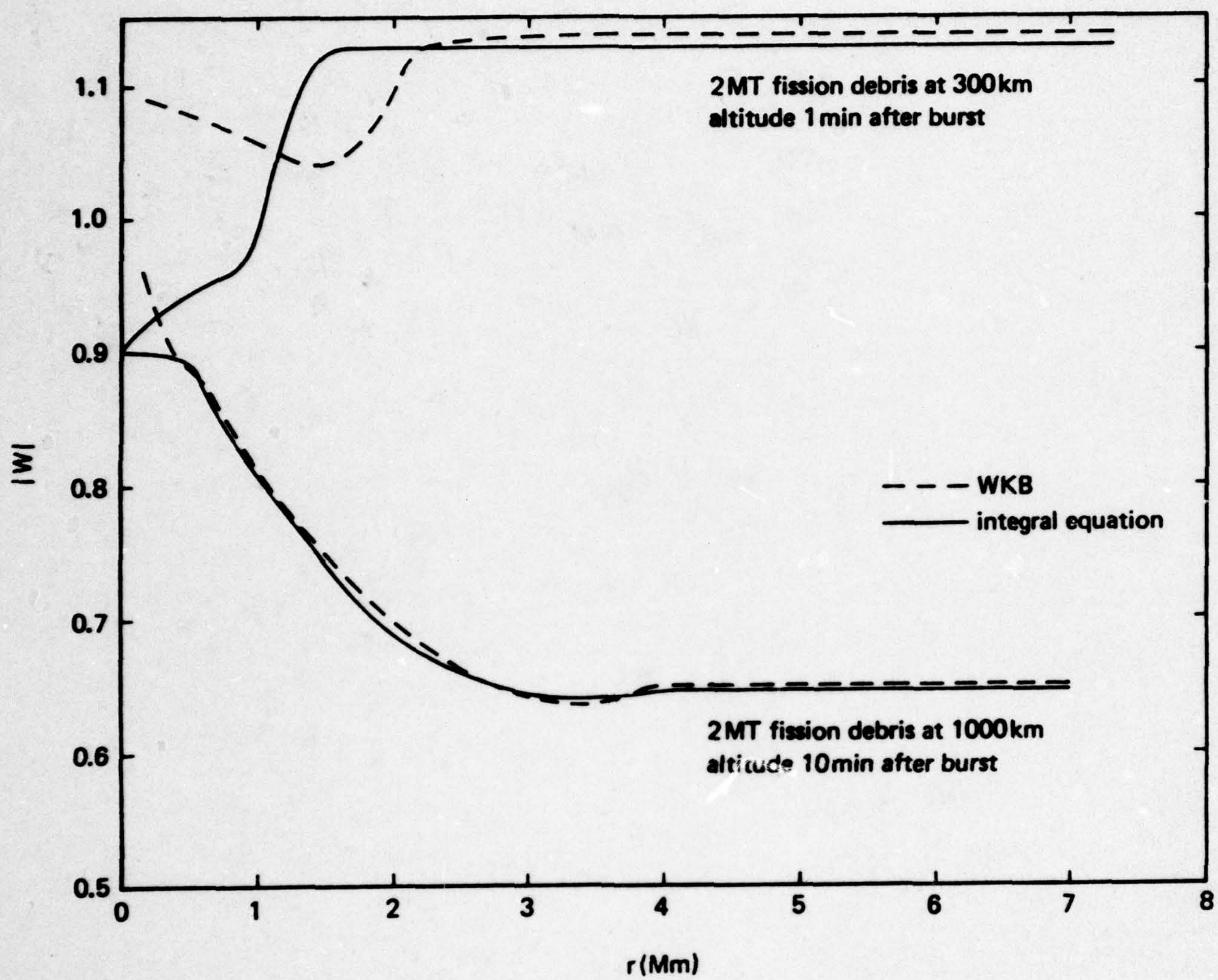

Fig. 9--Amplitude of W versus distance for two nominal nuclear disturbances over transmitter: daytime, f = 45 Hz.

IV. CONCLUSIONS

Recasting the equation for the lateral dependence of fields into an integral equation is a convenient means of obtaining numerical solutions for long-wave propagation under nonstratified conditions. The integral version accounts for most full-wave properties, including diffraction around a localized disturbance and reflection from lateral gradients. Numerical solutions based on model disturbances having lateral gradients in the direction of propagation reveal a standing wave pattern in front of the disturbance. The pattern is pronounced if the waveguide properties change substantially over a distance equal to about one-sixth of a wavelength, and is minor if the disturbance is more diffuse.

The often used WKB approximation of course ignores diffraction and gradient reflection. Thus it omits the standing wave pattern, thereby giving poor accuracy for regions in front of a disturbance having a relatively abrupt boundary. Because it ignores gradient reflections, the WKB approximation also overestimates the signal transmitted beyond a nonuniformity in the waveguide. However, for all models considered--abrupt or diffuse--the overestimate is minor.

The integral-equation method developed here is valid at any frequency for which waveguide modes describe terrestrial propagation. Nonetheless, its practical utility is probably limited to ELF since the lateral properties of the earth-ionosphere waveguide are usually gradual enough to permit use of the WKB approximation at higher frequencies.

Appendix A

INTEGRAL EQUATION FOR AN AZIMUTHALLY SYMMETRIC DISTURBANCE

If the disturbance is cylindrically symmetric and centered at the origin, $S^2(r) - S_0^2 = F(r)$, and Eq. (9) (p. 7) can be rewritten

$$\psi(r,\theta) = \psi_0(r,\theta) - \frac{ik^2}{4}\int_0^\infty r'dr'F(r')\int_0^{2\pi} d\theta' H_0^{(2)}(kS_0r_2)\psi(r',\theta') \quad , \qquad \text{(A-1)}$$

where r and θ are the usual circular cylindrical coordinates, and

$$r_2^2 = (r')^2 + r^2 - 2rr' \cos(\theta' - \theta) \quad . \qquad \text{(A-2)}$$

To obtain a one-dimensional integral equation in the variable r, we expand the terms in Eq. (A-1) in powers of $\cos\theta$ as follows:

$$\psi(r,\theta) = \sum_{m=0}^{\infty} \varepsilon_m \psi_m \cos m\theta \quad , \qquad \text{(A-3)}$$

$$H_0^{(2)}(kS_0r_2) = \sum_{n=0}^{\infty} \varepsilon_n \left\{ J_n(kS_0r_<)\, H_n^{(2)}(kS_0r_>) \right\} \cos n(\theta' - \theta) \quad , \qquad \text{(A-4)}$$

$$\psi_0(r,\theta) = S_0 H^{(2)}(kS_0r) \cos\theta \quad , \qquad \text{(A-5)}$$

where $\varepsilon_n = 1$ or 2 for $n = 0$ or $n \geq 1$, respectively, and $r_<$ and $r_>$ denote, respectively, the lesser or greater of r and r'. Equation (A-4) is the addition theorem for Hankel functions (e.g., *Magnus and Oberhettinger, 1943*), and Eq. (A-5) is the well-known solution for a laterally homogeneous, undisturbed ionosphere (see Eq. (3), p. 4).

By inserting Eqs. (A-3) through (A-5) into Eq. (A-1), and noting that

$$\int_0^{2\pi} d\theta' \cos n\theta' \cos m(\theta' - \theta) = \begin{cases} \pi \cos\theta & \text{if } n = m \\ 0 & \text{if } n \neq m \end{cases} , \quad \text{(A-6)}$$

it follows that

$$\sum_{m=0}^{\infty} \varepsilon_m \psi_m \cos m\theta = S_0 H_1^{(2)}(kS_0 r) \cos\theta - \frac{i\pi k^2}{4} \cos\theta \sum_{m=0}^{\infty} \varepsilon_m^2 \int_0^{\infty} r'dr'F(r')$$

$$\cdot J_m(kS_0 r_<) H_m^{(2)}(kS_0 r_>) \psi_m(r') \quad . \quad \text{(A-7)}$$

Using trigonometric orthogonality relations, it can be shown that only ψ_1 is nonzero, and the equation for the radial dependence of ψ becomes

$$\psi_1(r) = S_0 H_1^{(2)}(kS_0 r) - \frac{i\pi k^2}{2} \int_0^{\infty} r'dr'F(r') \, J_1(kS_0 r_<) H_1^{(2)}(kS_0 r_>) \psi_1(r') \quad . \quad \text{(A-8)}$$

The relative propagation function, W, is defined by

$$\psi(r) = \psi_0(r) W(r) \quad , \quad \text{(A-9)}$$

and combining Eqs. (A-3), (A-5), (A-8), and (A-9) gives the following result:

$$W(r) = 1 - \frac{i\pi k^2}{2} \int_0^{\infty} r'dr'F(r') \frac{J_1(kS_0 r_<) H_1^{(2)}(kS_0 r_>) H_1^{(2)}(kS_0 r')}{H_1^{(2)}(kS_0 r)} W(r') \quad . \quad \text{(A-10)}$$

Aside from some differences in notation, Eq. (A-10) is identical to Eq. (13) (p. 9).

Appendix B

WKB SOLUTION FOR AN AZIMUTHALLY SYMMETRIC DISTURBANCE

If S depends only on the distance, r, from the origin, Eq. (5) can be written

$$\frac{d^2}{dr^2}\psi + \frac{1}{r}\frac{d\psi}{dr} + (k^2S^2(r) - 1/r^2)\psi = 0 \quad . \tag{B-1}$$

By making substitution $\psi = u/r^{1/2}$, Eq. (B-1) can be transformed into the following standard form:

$$\frac{d^2u}{dr^2} + k^2\left[S^2(r) - \frac{3}{4k^2r^2}\right]u = 0 \quad . \tag{B-2}$$

If $S >> 1/kr$, Eq. (B-2) is identical to the equation of a plane wave propagating in a medium of refractive index S, and the WKB solution normalized to the definition of ψ given in Eqs. (3) and (4) can be written (e.g., *Budden, 1961b*):

$$\psi = u/r^{1/2} \sim \frac{S(r = 0)}{r^{1/2}\, S^{1/2}_{(r)}} \exp\left[-ik\int_0^r S(r')dr'\right] \quad . \tag{B-3}$$

Using the definition $W = \psi/\psi_0$, the WKB approximation to the relative propagation function is found to be

$$W(r)_{WKB} = \frac{S(r = 0)}{\left[S_0\ S(r)\right]^{1/2}} \exp\left[-ik\int_0^r [S(r') - S_0)]dr'\right] \quad , \tag{B-4}$$

which is Eq. (14) (p. 9).

REFERENCES

Budden, K. G., *The Waveguide Mode Theory of Wave Propagation*, Logos Press, London, 1961a.

-----, *Radio Waves in the Ionosphere*, University Press, Cambridge, 1961b.

Field, E. C., "The Effects of Ions on Very-Low-Frequency Propagation During Polar Cap Absorption Events," *Radio Science*, Vol. 5, March 1970, pp. 591-600.

-----, *ELF Propagation in a Non-Stratified Earth-Ionosphere Waveguide*, Pacific-Sierra Research Corp., Santa Monica, California, PSR 806, April 1978.

Field, E. C., and R. D. Engel, "The Detection of Daytime Nuclear Bursts Below 150 km by Prompt VLF Phase Anomalies," *Proc. IEEE*, Vol. 53, December 1965, pp. 2009-2017.

Galejs, J., *Terrestrial Propagation of Long Electromagnetic Waves*, Pergamon Press, New York, 1972.

Greifinger, C., and P. Greifinger, *Effects of a Cylindrically-Symmetric Ionospheric Disturbance on ELF Propagation in the Earth-Ionosphere Waveguide*, R&D Associates, Marina del Rey, California, DNA 43394, 10 June 1977.

-----, "Approximate Method for Determining ELF Eigenvalues in the Earth-Ionosphere Waveguide," *Radio Science*, Vol. 13, September-October 1978, pp. 831-837.

Hufford, G. A., "An Integral Equation Approach to the Problem of Wave Propagation Over an Irregular Surface," *Quart. Appl. Math.*, Vol. 9, 1952, pp. 391-403.

Magnus, W., and F. Oberhettinger, *Functions of Mathematical Physics*, Chelsea Publishing Co., New York, 1949.

Pappert, R. A., and W. F. Moler, "Propagation Theory and Calculations at Lower Extremely Low Frequencies (ELF)," *IEEE Trans. on Communications*, Vol. COM-22, April 1974, pp. 438-451.

Wait, J. R., "On Phase Changes in Very-Low-Frequency Propagation Induced by an Ionospheric Depression of Finite Extent," *Journ. of Geophys. Res.*, Vol. 59, No. 3, 1 February 1964, pp. 441-445.

-----, *Electromagnetic Waves in Stratified Media*, Pergamon Press, New York, 1970.

DISTRIBUTION LIST

Department of Defense

Director
Defense Advanced Research Projects Agency
1400 Wilson Boulevard
Arlington, Virginia 22209

1 cy ATTN: TIO
1 cy ATTN: STO
1 cy ATTN: NRMO

Director
Defense Communications Agency
8th Street and South Courthouse Road
Arlington, Virginia 22204

3 cys ATTN: MEECN Office

Defense Documentation Center
Cameron Station
Alexandria, Virginia 22314

12 cys ATTN: TC

Director
Defense Nuclear Agency
Washington, D. C. 20305

1 cy ATTN: STTL
1 cy ATTN: DDST
3 cys ATTN: RAAE
1 cy ATTN: RAEV

Joint Chiefs of Staff
Department of Defense
Washington, D. C. 20301

1 cy ATTN: J-6

Director
National Security Agency
Fort George G. Meade, Maryland 20755

2 cys ATTN: Technical Library

Undersecretary of Defense (Research and Engineering)
Department of Defense
Washington, D. C. 20301

2 cys ATTN: DDS&SS

Department of Commerce

U. S. Department of Commerce
Office of Telecommunications
Institute for Telecommunication Sciences
National Telecommunications and Information Administration
Boulder, Colorado 80303

2 cys ATTN: W. F. Utlaut

Department of the Army

Commander/Director
Atmospheric Sciences Laboratory
U. S. Army Electronics Command
White Sands Missile Range, New Mexico 88002

1 cy ATTN: DRSEL-BL-SY-S
F. E. Niles

Director
U. S. Army Ballistic Research Laboratories
Aberdeen Proving Grounds, Maryland 21005

1 cy ATTN: George E. Keller

Commander
U. S. Army Foreign Sciences and Technology Center
220 7th Street, N.E.
Charlottesville, Virginia 22901

1 cy ATTN: Robert Jones

Department of the Navy

Chief of Naval Operations
Department of the Navy
Washington, D. C. 20350

1 cy ATTN: NOP 985
1 cy ATTN: NOP 094H

Chief of Naval Research
Department of the Navy
800 North Quincy Street
Arlington, Virginia 22217

1 cy ATTN: Code 465, R. G. Joiner
1 cy ATTN: Code 427, H. Mullaney

Commander
Naval Electronic Systems Command
Department of the Navy
Washington, D. C. 20360

1 cy ATTN: PME-117
1 cy ATTN: PME-117T
1 cy ATTN: PME-117-21
1 cy ATTN: PME-117-21A
1 cy ATTN: PME-117-22

Director
Naval Ocean Systems Center
Electromagnetic Propagation Division
271 Catalina Boulevard
San Diego, California 92152

1 cy ATTN: Code 2200, W. F. Moler
1 cy ATTN: Code 2200, Richard Pappert
1 cy ATTN: Code 2200, John Bickel

Director
Naval Research Laboratory
4555 Overlook Avenue, S.W.
Washington, D. C. 20375

1 cy ATTN: Code 7700, Timothy P. Coffey
1 cy ATTN: Code 7709, Wahab Ali
2 cys ATTN: Code 7750, John Davis

Commander
Naval Surface Weapons Center (White Oak)
Silver Spring, Maryland 20910

1 cy ATTN: Technical Library

Office of Naval Research Branch Office (Pasadena)
1030 East Green Street
Pasadena, California 91106

1 cy

Department of the Air Force

Commander
Air Force Geophysical Laboratory, AFSC
L. G. Hanscom Air Force Base, Massachusetts 01731

1 cy ATTN: OPR, James Ulwick
1 cy ATTN: LKB, W. Swider
1 cy ATTN: LKB, K. Champion

Director
Air Force Technical Applications Center
Patrick Air Force Base, Florida 32920

1 cy ATTN: TD
1 cy ATTN: HQ 1035th TCHOG/TFS

Department of Defense Contractors

General Electric Company
TEMPO - Center for Advanced Studies
816 State Street
Santa Barbara, California 93102

1 cy ATTN: Warren S. Knapp
1 cy ATTN: DASIAC

Lockheed Missiles and Space Company
3251 Hanover Street
Palo Alto, California 94304

1 cy ATTN: J. B. Reagan
1 cy ATTN: W. Imhof
1 cy ATTN: Martin Walt

Mission Research Corporation
735 State Street
Santa Barbara, California 93101

1 cy ATTN: M. Scheibe
1 cy ATTN: D. Sowle

Pacific-Sierra Research Corporation
1456 Cloverfield Boulevard
Santa Monica, California 90404

1 cy ATTN: E. C. Field

Pennsylvania State University
Ionospheric Research Laboratory
College of Engineering
318 Electrical Engineering - East Wing
University Park, Pennsylvania 16802

1 cy ATTN: John S. Nisbet
1 cy ATTN: Les Hale
1 cy ATTN: A. J. Ferraro
1 cy ATTN: H. S. Lee

R&D Associates
4640 Admiralty Way
Marina Del Rey, California 90291

1 cy ATTN: R. Lelevier
1 cy ATTN: F. Gilmore
1 cy ATTN: R. Turco

The Rand Corporation
1700 Main Street
Santa Monica, California 90406

1 cy ATTN: Cullen Crain

Professor Chalmers F. Sechrist
155 Electrical Engineering Building
University of Illinois
Urbana, Illinois 61801

1 cy ATTN: C. Sechrist

Stanford Research Institute
333 Ravenswood Avenue
Menlo Park, California 94025

1 cy ATTN: Allen M. Peterson
1 cy ATTN: Ray L. Leadabrand

University of California, San Diego
Applied Physics and Information Science
La Jolla, California 92093

1 cy ATTN: Professor Henry Booker